JOURNAL OF CATALYSIS **172,** 13–23 (1997)
ARTICLE NO. CA971857

# Reaction and Surface Characterization Study of Higher Alcohol Synthesis Catalysts

## II. Cs-Promoted Commercial Zn/Cr Spinel

William S. Epling,* Gar B. Hoflund,*,[1] Walter M. Hart,† and David M. Minahan†

*Department of Chemical Engineering, University of Florida, Gainesville, Florida 32611; and †Union Carbide Corporation, Technical Center/P.O. Box 8361, South Charleston, West Virginia 25303

Received October 10, 1996; revised July 31, 1997; accepted July 31, 1997

**An Engelhard, Zn/Cr spinel, methanol-synthesis catalyst (Zn-0312) has been promoted with Cs and tested for isobutanol and methanol synthesis using a 1 : 1 CO and $H_2$ syngas feed stream. Two temperatures (400 and 440°C) and two pressures (1000 and 1500 psig) were tested, and the highest isobutanol product rates are attained using the higher temperature and pressure. Increasing the Cs-promotor concentration to 3 wt% decreases the hydrocarbon byproduct rate and increases the total alcohol production rate, alcohol selectivity, and isobutanol production rate. Above 3 wt% Cs, however, these values decrease as does the rate of hydrocarbon formation. A product isobutanol production rate of 116 g/kg-h can be attained using the 3 wt% Cs-containing catalyst at 440°C and 1500 psig. This production is greater than that obtained using a K-promoted Zn/Cr spinel catalyst indicating that the Cs is a better promotor for isobutanol production, which is consistent with previous findings. Surface-characterization studies performed on the 3 wt%-Cs-containing catalyst indicate that the near-surface region contains primarily ZnO with very little Cr. According to X-ray photoelectron spectroscopy (XPS) data, Cs is present as $Cs_2Cr_2O_7$ and maybe $Cs_2O$. These catalysts are reduced prior to tested in the reactor. Therefore, the catalyst was characterized after reduction in $1 \times 10^{-7}$ Torr of $H_2$ for 4 h at 250°C. Ion-scattering spectroscopy (ISS) data indicate that the outermost atomic layer of the as-prepared catalyst contains primarily C and O. Reduction results in enrichment of the outermost atomic layer with Cs, but smaller amounts of O, Na, Cl, Cr, and Zn also are present. While aging for 5 days in the reactor, the surface becomes O rich and the Zn-to-Cs atom ratio increases. These data suggest that Cs-promoted ZnO is the active catalyst phase and that neither Cr nor the spinel structure are required.** 

### INTRODUCTION

Methyl tertiary-butyl ether (MTBE) is an additive present in much of the unleaded gasoline today. This oxygenated additive acts as an octane-number enhancer and as an emission-reducing agent. MTBE can be derived from methanol to form the methyl portion and isobutylene to form the *t*-butyl fragment. Isobutylene is currently petroleum derived. Therefore, MTBE production can be feedstock limited depending upon the $C_4$ availability. An alternative reaction pathway using coal-derived syngas is possible, which would reduce this dependence. Syngas, ideally in stoichiometric proportion, can be used to produce isobutanol and methanol for downstream synthesis to MTBE, which is an existing technology. Low isobutanol productivities and poor alcohol distributions are obtained, however, using the best catalysts currently available. Improvements in the higher alcohol production catalysts are necessary in order for this reaction pathway to become economically viable.

The production of higher alcohols from syngas using alkali-promoted, methanol-synthesis catalysts has been studied extensively (1–18), although less attention has been given to the promoted high-pressure, high-temperature, zinc-chromite catalysts due to the more severe reaction conditions required. Nevertheless, these catalysts do have an advantage with regard to their greater selectivity for production of isobutanol. In the previous part of this study, a K promotor was added to an Engelhard Zn/Cr spinel, methanol-synthesis catalyst, and reaction and surface characterization studies were performed (18). Of the reaction conditions tested, the higher pressure, 1500 psig, and higher temperature, 440°C, result in the greatest isobutanol production. Increasing the amount of K in the catalyst lowers the hydrocarbon-byproduct rate, thereby increasing the selectivity to total alcohols. The use of a 3 wt% K-containing catalyst results in the highest isobutanol production as well as the lowest methanol-to-isobutanol mole ratio of 1.8. Ion scattering spectroscopy (ISS) studies reveal that the outermost surface layer of the fresh catalyst consists of C, O, Cr, and Zn. The catalysts were reduced prior to testing in the reactor so the catalysts were also characterized after a $1 \times 10^{-7}$ Torr $H_2$ exposure at 250°C for 4 h. After reduction

[1] Corresponding author.



0021-9517/97 $25.00

the outermost atomic layer consists of K. X-ray photoelectron spectroscopy (XPS) data indicate that the K and Cr are present as $K_2CrO_4$ or $K_2Cr_2O_7$. ZnO is the primary component of the near-surface regions of both the fresh and pretreated catalysts. The aged catalyst also is composed primarily of ZnO, but the chemical state of the Cr is altered to $Cr_2O_3$, $Cr(OH)_x$ and $Cr^0$ during the reaction. Although K is present at the outermost surface layer of the aged catalyst, little remains in the near-surface region according to the XPS data.

In the present study isobutanol production using a Cs-promoted, Engelhard Zn/Cr spinel, methanol synthesis catalyst has been examined. The nonpromoted Zn/Cr catalyst is commercially available and is advertised as a methanol synthesis catalyst. These catalysts are assumed to be optimized for methanol production so that the effects of Cs promotion on HAS can be directly monitored over a sample which catalyzes the production of a high volume of methanol. Two different operating pressures (1000 and 1500 psig) and two different operating temperatures (400 and 440°C) were used in order to examine the effects of temperature and pressure on catalyst performance for various Cs loadings. ISS and XPS were used to characterize the fresh, pretreated, and aged catalyst surfaces before and after depth profiling in order to ascertain chemical-state and compositional information regarding the near-surface regions of these samples. Morphological information from the fresh and aged catalyst surfaces was obtained using scanning electron microscopy (SEM).

## EXPERIMENTAL

The Zn/Cr spinel catalyst was purchased from Engelhard Industries (Zn 0312). The catalyst samples were impregnated with 1, 3, and 5 wt% Cs using the incipient wetness technique with cesium nitrate as the precursor. Each of these catalysts and the nonpromoted Zn/Cr spinel then were calcined in air at 350°C and pretreated in a 5% $H_2:N_2$ mixture prior to testing. The details of the reactor and characterization experiments have been described in detail previously (18). The surface area of the nonpromoted catalyst was determined to be approximately 80 $m^2/g$. SEM micrographs were taken using Scanning Electron Microscope Model SX-40A manufactured by International Scientific Instruments, Inc. The beam energy was kept constant at 15 keV at a magnification of 1,550.

## RESULTS AND DISCUSSION

The compositions of the product streams obtained using a nonpromoted 1, 3, and 5 wt% Cs-containing catalyst at four different sets of operating parameters and a 1:1 feed mixture of CO and $H_2$ are listed in Table 1. An increase in the reactor bed temperature results in an increase in the selectivity to total alcohols for all catalysts except for the 3 wt% Cs sample. This selectivity increase can be attributed to a sharp increase in the total alcohol production rate as the temperature is increased from 400 to 440°C. The isobutanol production rate is greatest when both the temperature and pressure are at the higher values tested. Furthermore, increasing the temperature at a pressure of 1500 psig decreases the methanol production rate resulting in lower methanol-to-isobutanol mole ratios. The highest isobutanol production rates consistently occur when the reactor is operated at 440°C and 1500 psi. Therefore, these conditions are the best settings of those tested for maximizing the isobutanol production rate. Similar results were reported using K-promoted Zn/Cr catalysts under identical reaction conditions (18). Unfortunately, the hydrocarbon by-product rate is greatest at these operating parameters as well. No significant changes in the product stream composition (i.e., no decay) were observed during the entire

**TABLE 1**

**Zn/Cr Engelhard Spinel Containing Four Different Operating Parameters**

| | 0 wt% Cs | | | | 1 wt% Cs | | | | 3 wt% Cs | | | | 5 wt% Cs | | | |
|---|---|---|---|---|---|---|---|---|---|---|---|---|---|---|---|---|
| P (psig) | 1000 | 1500 | 1500 | 1000 | 1000 | 1500 | 1500 | 1000 | 1000 | 1500 | 1500 | 1000 | 1000 | 1500 | 1500 | 1000 |
| T (°C) | 400 | 400 | 440 | 440 | 400 | 400 | 440 | 440 | 400 | 400 | 440 | 440 | 400 | 400 | 440 | 440 |
| Selectivity to total alcohols (%) | 65 | 77 | 43 | 27 | 62 | 76 | 57 | 75 | 87 | 91 | 81 | 83 | 97 | 98 | 76 | 62 |
| Total alcohol rate (g/kg-h) | 111 | 236 | 133 | 59 | 100 | 211 | 154 | 69 | 123 | 231 | 214 | 124 | 59 | 164 | 71 | 30 |
| Methanol rate (g/kg-h) | 105 | 223 | 102 | 41 | 48 | 119 | 32 | 11 | 56 | 138 | 48 | 18 | 48 | 139 | 27 | 8 |
| Ethanol rate (g/kg-h) | 0 | 0 | 0 | 0 | 0 | 0 | 0 | 0 | 0 | 0 | 10 | 2 | 0 | 0 | 0 | 0 |
| Isopropanol rate (g/kg-h) | 0 | 0 | 0 | 3 | 0 | 0 | 3 | 2 | 4 | 5 | 10 | 16 | 0 | 0 | 0 | 0 |
| *n*-Propanol rate (g/kg-h) | 0 | 0 | 18 | 10 | 0 | 0 | 5 | 2 | 13 | 21 | 20 | 16 | 0 | 0 | 8 | 5 |
| Isobutanol rate (g/kg-h) | 6 | 13 | 13 | 5 | 52 | 92 | 115 | 57 | 49 | 67 | 116 | 67 | 11 | 25 | 36 | 17 |
| MetOH/i-ButOH mole ratio | 73 | 68 | 31 | 36 | 3.8 | 5.2 | 1.1 | 0.8 | 4.6 | 8.2 | 1.7 | 1.1 | 17 | 23 | 3 | 1.9 |
| Hydrocarbon rate (g/kg-h) | 30 | 35 | 94 | 86 | 36 | 38 | 81 | 62 | 11 | 13 | 35 | 19 | 1 | 2 | 35 | 12 |
| Conversion (%) | 8 | 14 | 14 | 9 | 11 | 16 | 16 | 14 | 15 | 20 | 18 | 15 | 12 | 13 | 18 | 10 |

5-day test period including utilization of the higher temperature and pressure conditions.

The effect of Cs loading on the product stream composition was tested also. The total alcohol production rate as a function of promotor loading at 440°C and 1500 psig is shown in Fig. 1a. A maximum total alcohol production rate of 214 g/kg-h is achieved using the 3 wt% Cs-containing catalyst. Further addition of Cs to 5 wt%, however, results in a sharp decrease in the total alcohol production rate. The separate isobutanol and methanol production rates are shown in Fig. 1b. The addition of 1 wt% Cs to the spinel greatly increases the isobutanol production rate and decreases the methanol production rate. Increasing the Cs-promotor loading to 3 wt% results in a slight increase in the isobutanol production rate to 116 g/kg-h, but an increase in the methanol production rate occurs as well. This increases the methanol-to-isobutanol mole ratio from 1.1 to 1.7. Using the 5 wt% Cs-containing catalyst significantly decreases the isobutanol production rate which coincides with the sharp decrease in the total alcohol production rate mentioned above. The effect of Cs addition on the selectivity to total alcohols is shown in Fig. 2a. Promoting the spinel catalyst with Cs increases the selectivity toward total alcohol production, and a maximum occurs using the 3 wt% Cs-containing catalyst. As shown in Fig. 2b, increasing the amount of Cs results in a monotonic decrease of hydrocarbon byproduct rate. Hence, the selectivity decrease upon the addition of 5 wt% Cs is attributed solely to the decrease

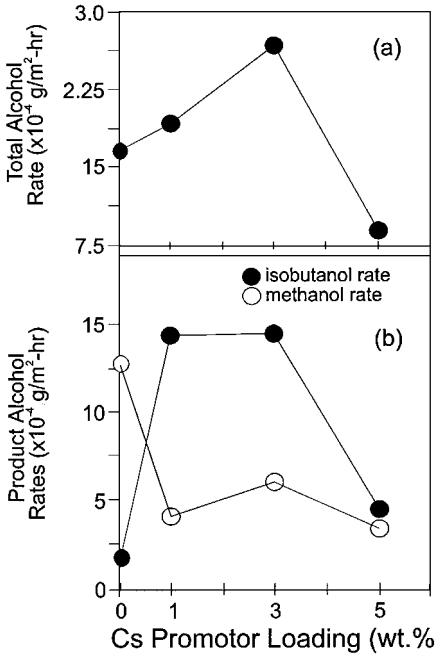


**FIG. 1.** The effect of Cs loading on (a) the total alcohol production rate and (b) the isobutanol and methanol production rates at 440°C and 1500 psig.

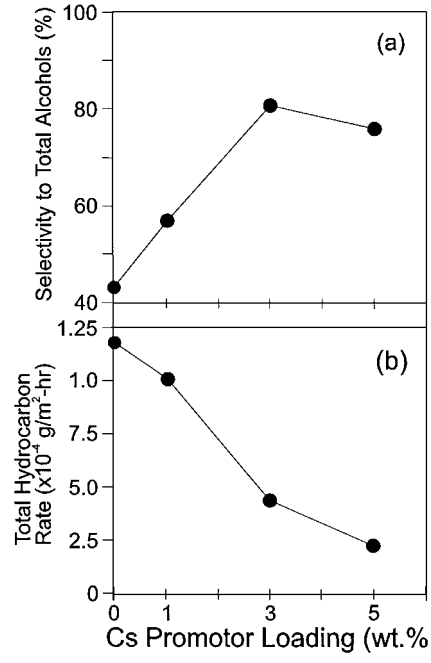


**FIG. 2.** The effect of Cs loading on (a) the selectivity to total alcohols and (b) the total hydrocarbon-byproduct rate at 440°C and 1500 psig.

in the isobutanol production rate. Overall, the addition of Cs results in improved catalyst performance upon comparison with the K-promoted catalysts (18). Greater total alcohol and isobutanol production rates and higher selectivities to alcohol are achieved using Cs as the promotor rather than K. Furthermore, lower methanol-to-isobutanol mole ratios can be obtained using the appropriate reaction conditions (18). Surface-science analysis was performed on the Zn/Cr spinel catalyst containing 3 wt% Cs because the highest isobutanol production rate, highest total alcohol production rate and greatest selectivity to alcohols is achieved using this catalyst.

An SEM micrograph obtained from the nonpromoted Zn/Cr spinel is shown in Fig. 3a. Large plate structures are stacked upon each other, and smaller rectangular structures cover the topmost plate. An SEM micrograph taken from the 3 wt% Cs-containing, Zn/Cr spinel is shown in Fig. 3b. The plate structures are now almost completely covered by a network of fiber-like structures, and small globular formations are spread randomly over the surface as well. The network of fibrous particles is not present in the SEM micrograph shown in Fig. 3c taken from the aged catalyst, but the small bead-like particles still cover the entire surface. The nonpromoted, spinel structure described as stacked plates also is apparent, although covered. The fibrous network is visible in the SEM micrographs obtained from the fresh and aged 3 wt% K-containing, Zn/Cr spinel as shown in Figs. 3d and 3e. On this catalyst the bead-like particles are larger and the spinel support seems to be fractured into smaller

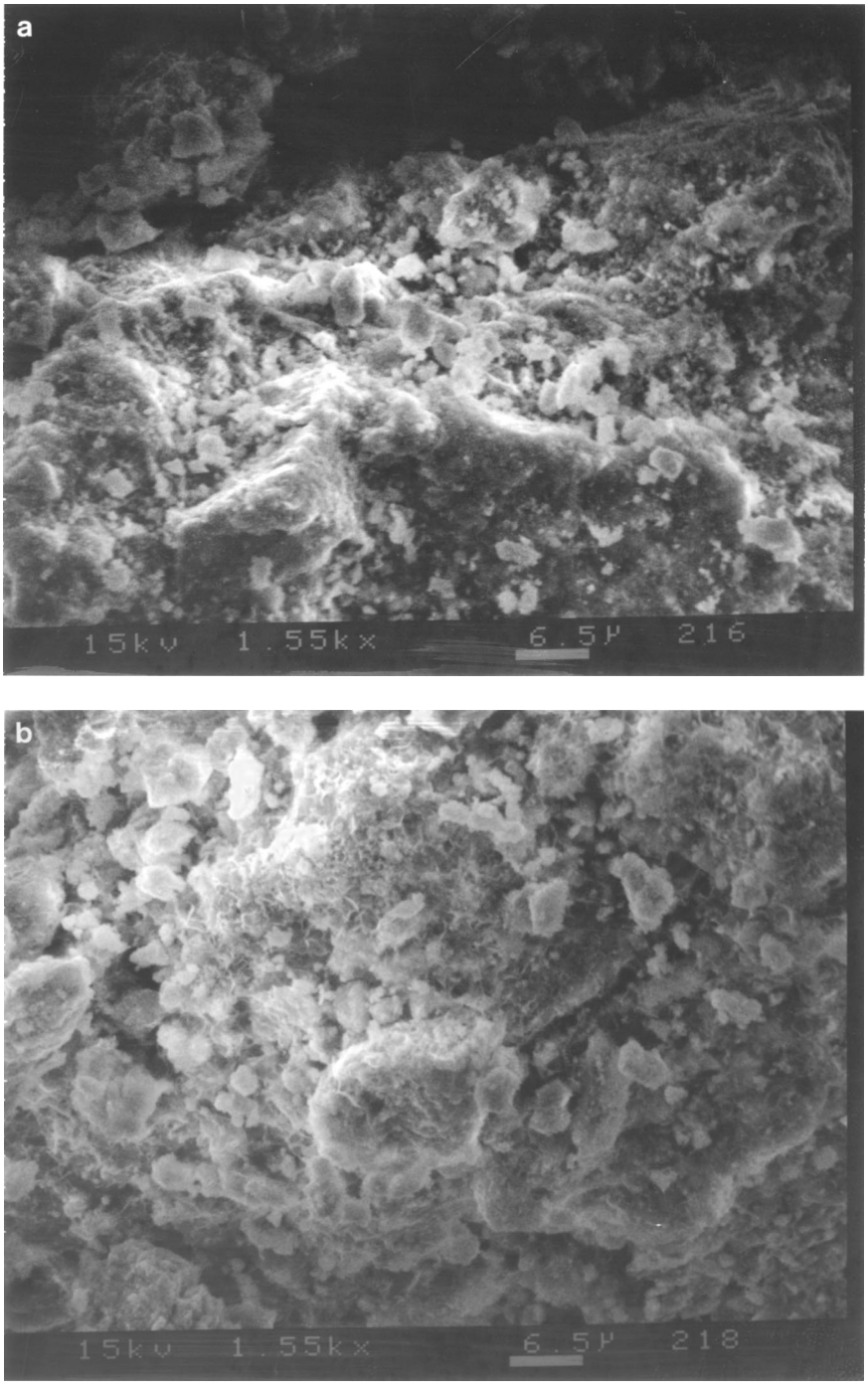


**FIG. 3.** SEM micrographs obtained from (a) the nonpromoted, Engelhard Zn/Cr spinel, (b) the fresh, (c) aged, 3 wt% Cs-promoted Zn/Cr spinel, (d) the fresh, and (e) the aged, 3 wt% K-containing Zn/Cr spinel.

plates. Furthermore, the network of fibrous particles does not disappear with pretreatment or catalyst aging as on the Cs-promoted catalyst.

The high surface sensitivity of ISS makes it a very useful surface analysis technique particularly when used in conjunction with less surface sensitive techniques such as XPS. ISS is capable of yielding compositional information about the outermost atomic layer of a sample. In catalysis this is very important since the chemical reactions occur at the outermost catalyst surface. An ISS spectrum taken from the fresh 3 wt% Cs-containing catalyst is shown in Fig. 4a. A large feature is present at an $E/E_0$ value of approximately

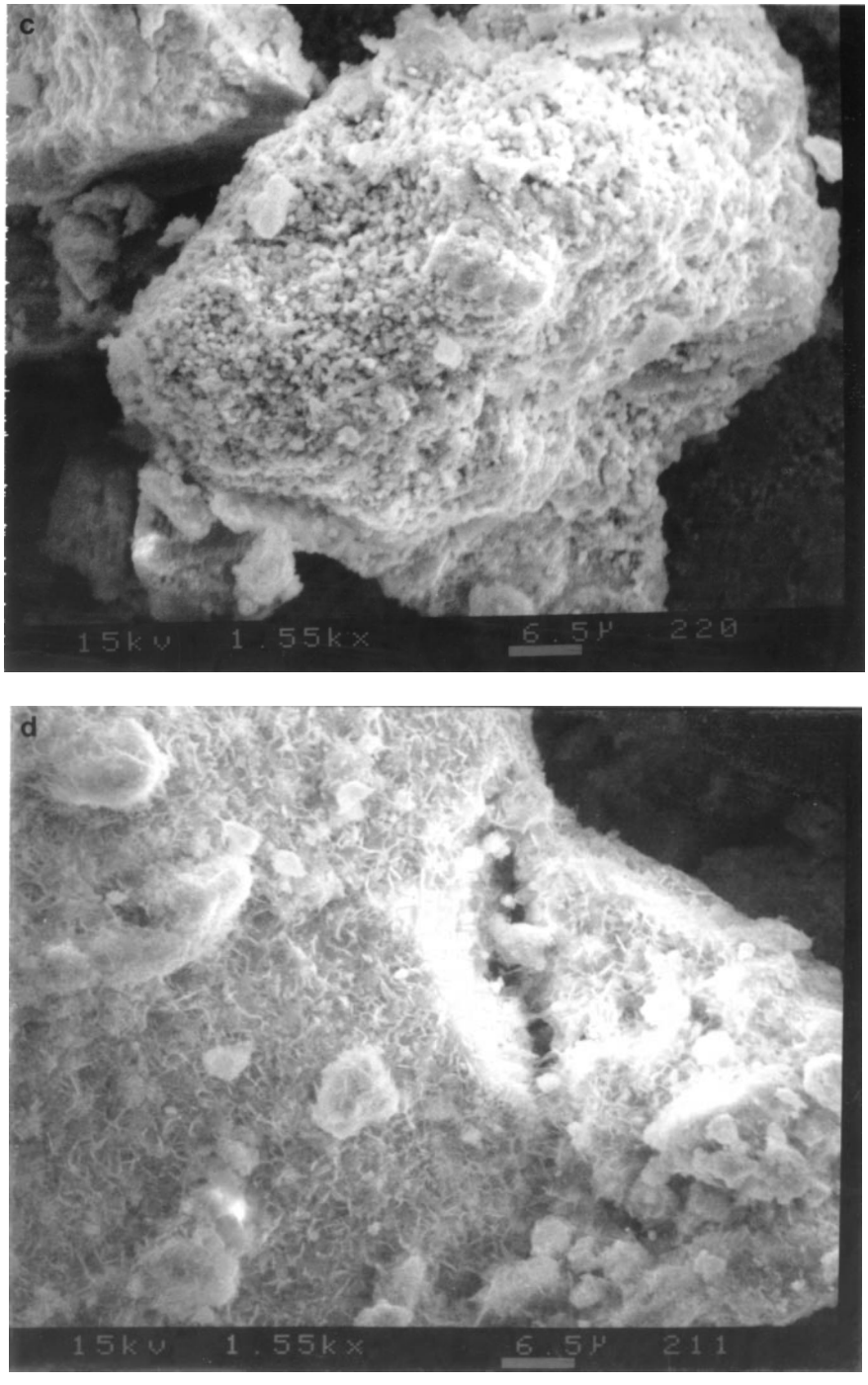


**FIG. 3**—*Continued*

0.34 due to C, and a shoulder is present at an $E/E_0$ of 0.42 due to O. These values are higher than predicted by the elastic binary scattering equation due to charging as evidenced by the low-energy feature at an $E/E_0$ of 0.18. Upon expanding the region between $E/E_0$ values of 0.74 and 0.96 by a factor of 5, features due to the presence of Cs and Zn are observable. The spectrum shown in Fig. 4b was taken from the 3 wt% Cs-promoted catalyst after exposure to $1 \times 10^{-7}$ Torr of $H_2$ for 4 h at 250°C which is similar to the pretreatment used on the catalysts before reaction studies. The charging feature remains at an $E/E_0$ of about 0.2 but is diminished in size. A large Cs peak is evident and Zn and Cr features are also present, but they are much smaller than the Cs peak. Na and Cl contaminants are present on this

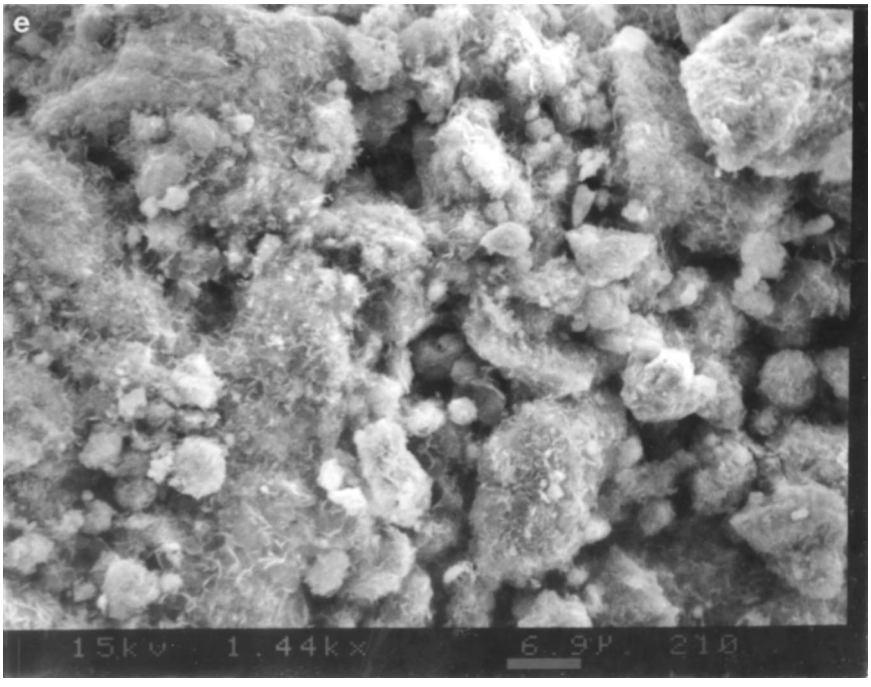


**FIG. 3**—*Continued*

surface also. The O feature is small, but due to the low cross section of O in ISS, this small signal still indicates that a significant surface concentration of oxygen is present. After sputtering the pretreated catalyst for 5 min with 1-keV $He^+$, the spectrum shown in Fig. 4c was taken. The Zn feature is increased in size relative to the Cs peak indicating that Cs removal exposes underlying Zn, and the Cr feature is larger than in Fig. 4b. The Cl peak is no longer evident and the Na feature may be somewhat decreased. After sputtering the sample for an additional 15 min with 1-keV 1:1 $He^+$ and $Ar^+$, the spectrum shown in Fig. 4d was obtained. The Cs peak is now relatively small, and the Zn and Cr features are increased in size. Furthermore, the background signal is diminished indicating that the surface is more conductive or less oxidic as evidenced by the lack of an O feature at an $E/E_0$ of 0.37. This series of ISS spectra closely resemble those taken from the K-promoted catalyst presented in the earlier study (18) in which the outermost surface layer of the fresh catalyst is composed primarily of oxygen and a reductive pretreatment results in coverage of the surface with K. These results demonstrate that the reductive treatment enriches the surface in the alkali promotor and reduces the amount of carbon contamination which may expose active catalytic sites.

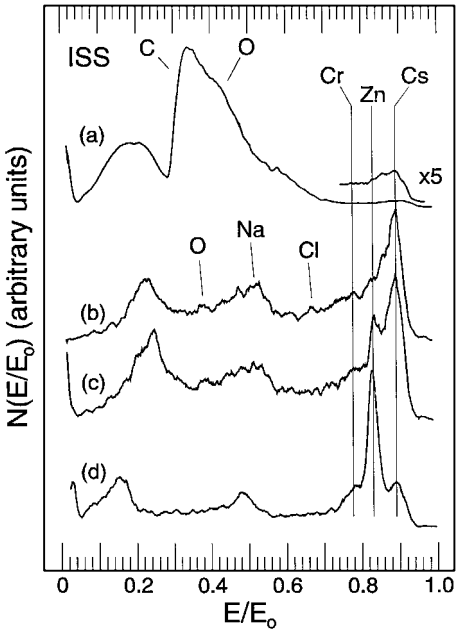


**FIG. 4.** ISS spectra obtained from the 3 wt% Cs-promoted Zn/Cr spinel catalyst after (a) insertion into the UHV system, (b) pretreatment in $1 \times 10^{-7}$ Torr of $H_2$ for 4 h at 250°C, (c) sputtering for 5 min with 1-keV $He^+$, and (d) sputtering for another 15 min with 1-keV 1:1 $He^+$ and $Ar^+$.

Surface analysis also was performed on the catalysts after exposure to the reactant stream for 5 days. An ISS spectrum taken from an aged, 3 wt% Cs catalyst is shown in Fig. 5a. Again, a large charging feature is apparent at the lower $E/E_0$ values which indicates the outermost surface layer contains substantial amounts of oxygen and carbon. Cs and Zn features are present, and the Cs-to-Zn peak-height ratio is not significantly different from that obtained from the pretreated catalyst (Fig. 4b). A small amount of Cl also is apparent at the surface of the aged catalyst. After

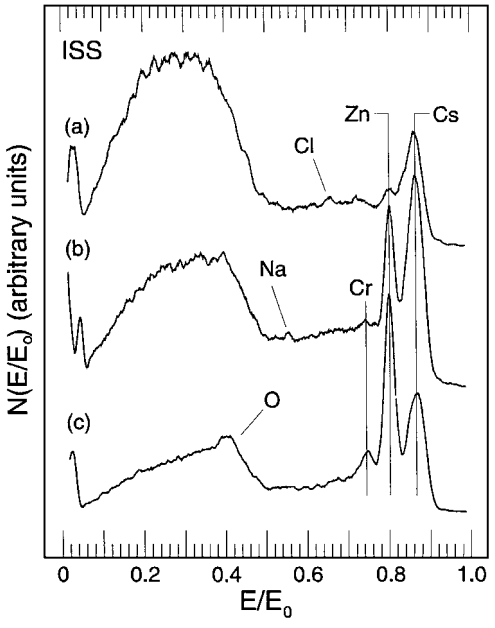


**FIG. 5.** ISS spectra obtained from the aged, 3 wt% Cs-promoted Zn/Cr spinel catalyst after (a) insertion into the UHV system, (b) sputtering for 5 min 1-keV $He^+$, and (c) sputtering for another 15 min with 1-keV 1:1 $He^+$ and $Ar^+$.

sputtering the sample for 5 min, the ISS spectrum shown in Fig. 5b was taken. The Zn-to-Cs peak-height ratio is increased significantly, and a small Na peak due to sample contamination is present. Although a Cr feature is apparent, it is quite small in comparison to the Zn peak. Further sputtering of the sample results in a significant decrease in the Cs peak intensity and an increase in both the Zn and Cr features as shown in Fig. 5c indicating that Cs covers the underlying Zn and Cr. The Cs may be present as the bead-like structures which are evident in the SEM micrograph shown in Fig. 3c. The bead structures cover most of the catalyst surface although some bare patches are visible which accounts for the small signal Zn contribution before sputtering. The broad feature extending from an $E/E_0$ of 0.06 to 0.5 is due to the presence of C and O. These features decrease in size compared to the Zn feature with sputtering. This indicates that the surface layer of the aged catalyst contains large amounts of C and O compared to the pretreated catalyst (Fig. 4b). The changes in shape indicate that the C sputters away more rapidly leaving a better defined O peak. Another small peak is apparent in these ISS spectra at an $E/E_0$ below 0.06. This peak is composed of secondary ions which typically are mostly $H^+$.

An XPS survey spectrum obtained from the fresh, 3 wt% Cs catalyst is shown in Fig. 6. Features due to Zn, Cs, and O are readily apparent as are small $Cr_{2p}$ peaks. These XPS data and the ISS data indicate that the near-surface region of this sample is enriched in Zn. This result also is consistent with data obtained from the 3 wt% K-promoted Zn/Cr spinel catalyst (18). Similar survey spectra were obtained from the pretreated and aged catalysts so they are not presented. The most significant difference in the spectra is the size of the $Cr_{2p}$ peaks. The $Cr_{2p}$ peaks are larger after the fresh catalyst sample is reduced and after the aged catalyst is sputtered. These results are consistent with trends shown by the ISS data, but care must be taken in comparing ISS and XPS data because ISS is outermost atomic layer sensitive and XPS typically probes more than 30 atomic layers beneath the surface with less than 10% of the signal originating from the outermost atomic layer. Subsurface compositional changes detected by XPS may be quite different than outermost atomic layer compositional changes detected using ISS.

A high-resolution, $Zn_{2p}$ XPS spectrum taken from the fresh catalyst is shown in Fig. 7a. Based on the peak shape and width, ZnO apparently is the only chemical state of Zn present in the near-surface region of the as-prepared sample. X-ray diffraction (XRD) data obtained from the fresh catalyst indicates the presence of ZnO and $ZnCr_2O_4$. XRD, however, is not a surface sensitive characterization technique and only detects crystalline phases. Based on the XPS data shown in Fig. 7a, the $ZnCr_2O_4$ is beneath the ZnO layer since features due to $ZnCr_2O_4$ are not apparent. Therefore, the spinel acts as a support material and does not play a role in the catalytic reaction process. This ZnO feature also is the only peak present in the spectra taken from the pretreated and sputtered samples as shown in Figs. 7b and c. The $Zn_{2p}$ XPS spectrum taken from the aged catalyst, shown in Fig. 7d, contains two distinct features. The lower binding-energy (BE) peak is assigned as ZnO. The higher BE peak is due to sample charging since this feature lies beyond the BE range observed in XPS spectra

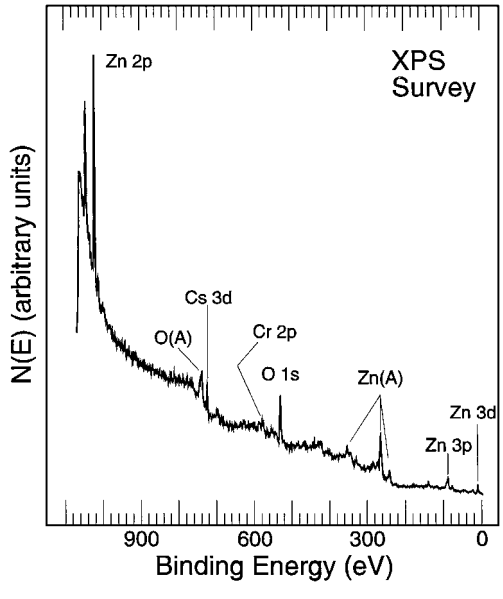


**FIG. 6.** XPS survey spectrum taken from the fresh, nonpretreated, 3 wt% Cs-promoted Zn/Cr spinel catalyst.

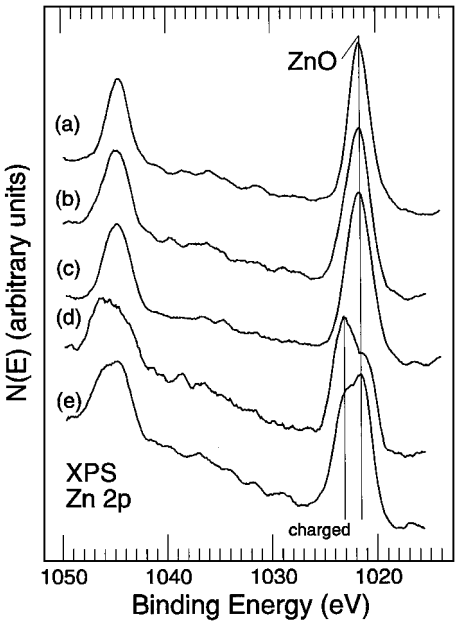


**FIG. 7.** High-resolution XPS $Zn_{2p}$ spectra taken from the 3 wt% Cs-promoted Zn/Cr spinel catalyst after (a) insertion into the UHV chamber, (b) pretreatment in $1 \times 10^{-7}$ Torr of $H_2$ at 250°C for 4 h, (c) sputtering the pretreated sample for 5 min with 1-keV $He^+$ and 15 min with 1-keV 1:1 $He^+$ and $Ar^+$, (d) insertion of the aged 3 wt% Cs-promoted Zn/Cr spinel catalyst into the UHV chamber, and (e) sputtering the aged catalyst for 5 min with 1-keV $He^+$ and for 15 min with 1-keV 1:1 $He^+$ and $Ar^+$.

taken from Zn compounds. Sputtering the aged catalyst reduces the intensity of the charging feature as shown in Fig. 7e suggesting that the charged feature is due to a ZnO phase which lies near to the surface. This charging feature probably was not present in the unreacted samples due to a greater or stronger interaction between the surface and bulk structures. The SEM data presented above shows beadlike structures lying atop the larger plates. These beadlike structures may interact less with the plates resulting in two separate layers being examined which would explain the two sets of features observed in these XPS spectra. This is consistent with the assertion that the charged region is at the surface. Peaks other than that due to ZnO would be difficult to detect due to the large intensity of the ZnO peak. Therefore, small amounts of other Zn compounds may be present, but are not distinguishable. ZnO was the only chemical state of Zn observed in the near-surface region of the K-promoted Zn/Cr spinel catalyst also (18). In a separate study by Campos-Martin *et al.* (19), ZnO again was the only state of Zn observed using XPS to examine a Zn/Cr spinel catalyst before and after a reductive treatment in a $H_2$ and $N_2$ mixture.

An XPS $O_{1s}$ spectrum obtained from the fresh catalyst is shown in Fig. 8a. Features due to the presence of several chemical states of oxygen are evident. The predominant peak is assigned as O in ZnO, and the small peak at approximately 527.3 eV is due to chemisorbed oxygen or possibly $Cs_2O$. A small shoulder is evident at 532.8 eV due to the presence of adsorbed water, and the broadening on the high BE side of the $O_{1s}$ peak indicates that hydroxyl groups are present. Reducing the catalyst at 250°C for 4 h in $1 \times 10^{-7}$ Torr of $H_2$ removes both the adsorbed water and chemisorbed oxygen or $Cs_2O$ as shown in Fig. 8b. This may result in a greater exposure of underlying active catalytic sites. A contribution by $OH^-$ results in the broadening toward the high BE side of this peak. After sputtering the pretreated catalyst for 5 min with 1-keV $He^+$ and for 15 min with 1-keV 1:1 $He^+$ and $Ar^+$, the spectrum shown in Fig. 8c was taken. The primary O state is due to ZnO, but hydroxyl groups which initially are beneath the probing depth of XPS are now exposed. An XPS $O_{1s}$ spectrum taken from the aged catalyst is shown in Fig. 8d. A ZnO feature is evident as is another feature 1.4 eV higher in BE. The charging features present in the $Zn_{2p}$ spectra taken from the aged catalyst are also higher in BE by 1.4 eV. Therefore, the predominant $O_{1s}$ peak is due to sample charging. Unfortunately, this makes the detection of other oxygen features difficult in both spectra shown in Figs. 8d and e, the spectrum obtained from the aged catalyst after sputtering. The features due to the presence of ZnO in the charged and subsurface regions are evident in the spectra taken from both samples. Sputtering results in a decrease in the charged

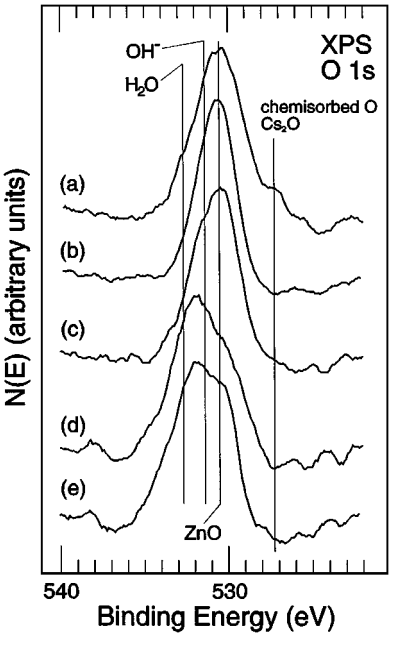


**FIG. 8.** High-resolution XPS $O_{1s}$ spectra taken from the 3 wt% Cs-promoted Zn/Cr spinel catalyst after (a) insertion into the UHV chamber, (b) pretreatment in $1 \times 10^{-7}$ Torr of $H_2$ at 250°C for 4 h, (c) sputtering the pretreated sample for 5 min with 1-keV $He^+$ and 15 min with 1-keV 1:1 $He^+$ and $Ar^+$, (d) insertion of the aged 3 wt% Cs-promoted Zn/Cr spinel catalyst into the UHV chamber, and (e) sputtering the aged catalyst for 5 min with 1-keV $He^+$ and for 15 min 1-keV with 1:1 $He^+$ and $Ar^+$.

$O_{1s}$ feature similar to the decrease in the charged $Zn_{3d}$ feature.

An XPS $C_{1s}$ spectrum obtained from the fresh catalyst is shown in Fig. 9a. A small feature, barely above the noise level, is apparent at 284.8 eV. This most likely is attributable to the presence of hydrocarbons on the catalyst surface which is typical of air-exposed samples. The $C_{1s}$ XPS spectrum taken after pretreating the sample in $1 \times 10^{-7}$ Torr of $H_2$ for 4 h at 250°C is shown in Fig. 9b. No C peaks are observable after sputtering the sample so this spectrum is not shown. The spectrum taken from the aged catalyst contains a large $C_{1s}$ peak as shown in Fig. 9c. This spectrum and the one taken from the aged catalyst after sputtering, shown in Fig. 9d, may be affected by the charging effect noted above thereby making chemical-state assignments difficult. Charging would account for the breadth of the two peaks and the decrease in intensity of the higher BE portion of the peak taken after sputtering. A predominant contribution to these features is due to hydrocarbons, and alcohols most likely contribute also. The presence of both is expected since they are reaction products. A smaller peak is present at a BE of 290.0 eV which is due to carbonates. This is shifted to a higher BE by 1.4 eV due to charging. These XPS data are consistent with the ISS data shown in Fig. 5 in which a carbonaceous layer containing O is removed during ISS depth profiling. These data further indicate that a carbon buildup occurs during the reaction process.

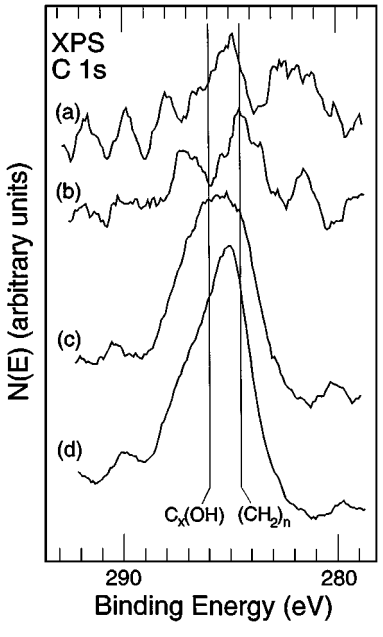


**FIG. 9.** High-resolution XPS $C_{1s}$ spectra taken from the 3 wt% Cs-promoted Zn/Cr spinel catalyst after (a) insertion into the UHV chamber, (b) pretreatment in $1 \times 10^{-7}$ Torr of $H_2$ at 250°C for 4 h, (c) sputtering the pretreated sample for 5 min with 1-keV $He^+$ and 15 min with 1-keV 1 : 1 $He^+$ and $Ar^+$, (d) insertion of the aged 3 wt% Cs-promoted Zn/Cr spinel catalyst into the UHV chamber, and (e) sputtering the aged catalyst for 5 min with 1-keV $He^+$ and for 15 min with 1 : 1 $He^+$ and $Ar^+$.

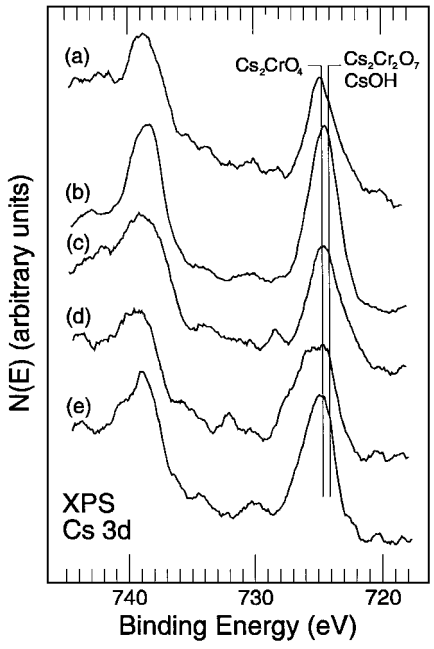


**FIG. 10.** High-resolution XPS $Cs_{3d}$ spectra taken from the 3 wt% Cs-promoted Zn/Cr spinel after (a) insertion into the UHV chamber, (b) pretreatment in $1 \times 10^{-7}$ Torr of $H_2$ at 250°C for 4 h, (c) sputtering the pretreated sample for 5 min with 1-keV $He^+$ and 15 min with 1-keV 1 : 1 $He^+$ and $Ar^+$, (d) insertion of the aged 3 wt% Cs-promoted Zn/Cr spinel catalyst into the UHV chamber, and (e) sputtering the aged catalyst for 5 min with 1-keV $He^+$ and for 15 min with 1 : 1 $He^+$ and $Ar^+$.

The XPS $Cs_{3d}$ spectrum taken from the fresh catalyst is shown in Fig. 10a. The predominant peak lies at a BE value of approximately 724.7 eV indicating that the Cs is present as $Cs_2CrO_4$ (19). $Cs_2O$ has a similar BE value but is not typically considered a stable state of Cs in a vacuum environment. The ZnO, however, may stabilize this state, allowing it to be present in the near-surface region. A shoulder is also evident at 724.0 eV which is assigned as due to $Cs_2Cr_2O_7$ (20). CsOH has a very similar BE at 724.15 eV (21) and may also contribute to the intensity of this peak. The Cs promotor was added to the catalyst as cesium nitrate. No $N_{1s}$ signal is apparent in the survey spectrum obtained from the fresh catalyst (Fig. 6) indicating that the precursor material reacted with the Zn/Cr sample forming the chemical species observed and releasing the N. The $Cr_{2p}$ XPS spectrum taken from the fresh catalyst, shown in Fig. 11a, also contains a feature due to the presence of $Cs_2Cr_2O_7$ at 579.3 eV and a shoulder at a BE of 579.8 due to the presence of $Cs_2CrO_4$ (22). Features due to the presence of other Cr states such as $Cr_2O_3$, $Cr(OH)_x$, and $CrO_2$ are present as well. Although $CrO_2$ is typically not considered a stable chemical state of Cr, it is observed in the near-surface region of polycrystalline Ni/Cr samples (23). In this study the $CrO_2$ is most likely stabilized by the matrix or ZnO near the surface. The XPS $Cs_{3d}$ and $Cr_{2p}$ spectra obtained after reducing the sample are shown in Figs. 10b and 11b,

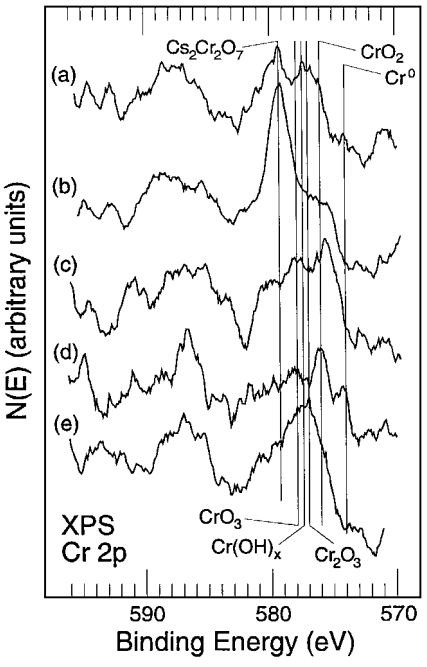


**FIG. 11.** High-resolution XPS $Cr_{2p}$ spectra taken from the 3 wt% Cs-promoted Zn/Cr spinel after (a) insertion into the UHV chamber, (b) pretreatment in $1 \times 10^{-7}$ Torr of $H_2$ at 250°C for 4 h, (c) sputtering the pretreated sample for 5 min with 1-keV $He^+$ and 15 min with 1-keV 1:1 $He^+$ and $Ar^+$, (d) insertion of the aged 3 wt% Cs-promoted Zn/Cr spinel catalyst into the UHV chamber, and (e) sputtering the aged catalyst for 5 min with 1-keV $He^+$ and for 15 min with 1-keV 1:1 $He^+$ and $Ar^+$.

respectively. The predominant $Cs_{3d}$ feature is due to a mixture of cesium dichromate and cesium chromate although more cesium dichromate is now present. It is larger than the peak shown in Fig. 10a as is the primary $Cr_{2p}$ peak which is also due to the presence of cesium dichromate. Similar to observations made after pretreating K-containing catalysts (18), the reductive treatment removes surface O and causes a reaction between Cr and Cs to form $Cs_2Cr_2O_7$. Although XPS probes more deeply than ISS, these results are consistent with the ISS results discussed above which indicate that the outermost layer is composed primarily of Cs after the reductive pretreatment. These data further demonstrate that the reductive pretreatment enriches the surface region in the alkali promotor which is necessary for HAS. As shown in Figs. 10c and 11c, sputtering the sample results in a decrease of the Cs concentration and an alteration in the Cr chemical states to a mixture of oxides. The $Cs_{3d}$ spectra taken from the aged catalyst before and after sputtering, shown in Figs. 10d and e, respectively, are affected by sample charging. Features due to $Cs_2CrO_4$, $Cs_2Cr_2O_7$, and CsOH are evident, and the feature due to charging is sputtered away more quickly than those associated with the $Zn_{2p}$ and $O_{1s}$ spectra. This may indicate that most of the Cs is located nearer to the surface and not evenly dispersed through the bulk of the sample which also is consistent with the ISS data. The $Cr_{2p}$ XPS spectrum taken from the aged catalyst, shown in Fig. 11d, contains a mixture of features, most of which are barely discernible above the background. $CrO_2$ is apparently the predominant feature. Sputtering the aged catalyst results in the exposure of more distinct $Cr_{2p}$ features as shown in Fig. 11e. Signal contributions due to the presence of $Cr(OH)_x$, $CrO_2$, $CrO_3$, $Cr_2O_3$, and $Cs_2Cr_2O_7$ are evident.

## CONCLUSIONS

A commercially available Zn/Cr spinel, methanol-synthesis catalyst (Engelhard Zn-0312) was promoted with various amounts of Cs and tested for isobutanol and methanol synthesis. The highest isobutanol production rates were achieved using the higher temperature and higher pressure settings of 440°C and 1500 psi. However, these reaction conditions also result in the higher hydrocarbon byproduct rates. The total alcohol production rate and the selectivity to total alcohols and isobutanol production rate increase upon adding Cs and attain a maximum with the addition of 3 wt% Cs. The hydrocarbon by-product rate decreases with increasing Cs concentration. The results indicate that a better catalyst for the production of an equimolar mixture of isobutanol and methanol can be achieved by promoting the Zn/Cr spinel with Cs rather than K. Lower methanol-to-isobutanol mole ratios can be obtained as well as higher isobutanol production rates. The near-surface region of the fresh catalyst consists primarily of ZnO, $Cs_2Cr_2O_7$, and possibly some $Cs_2O$. SEM micrographs of the fresh catalyst show that a fibrous network of particles exists over the Zn/Cr spinel, plated structure. A reductive pretreatment removes O exposing Cs, which almost completely covers the ZnO. The Cs is predominantly in the form of $Cs_2O$ in the fresh catalyst, but after the reductive pretreatment $Cs_2Cr_2O_7$ is the primary chemical state of Cs in the near-surface region. Less Cs and Cr is present in the near-surface region of the aged catalyst which was removed from the reactor after a 5-day test period. The outermost atomic layer of the aged catalyst consists primarily of Cs and a small amount of Cl. The near-surface region of the aged catalysts contains primarily ZnO. The Cr close to the surface is present as $CrO_2$ and $Cr^0$ while subsurface Cr is present primarily as $Cr_2O_3$, $Cr(OH)_x$, and $CrO_3$. The morphology of the catalyst changes with age. The fibrous particles are not evident on the aged catalyst, but small bead-like particles cover most of the underlying Zn/Cr spinel structure.

## ACKNOWLEDGMENTS

The authors appreciate assistance from Pete Axson with regard to obtaining the SEM micrographs. Financial support for this research was provided by the National Science Foundation through Grant CTS-9122575 and the Department of Energy through Contract DE-AC22-91PC90046.

## REFERENCES


1. Satterfield, C. N., "Heterogeneous Catalysis in Industrial Practice," 2nd ed., p. 454. McGraw-Hill, New York, 1991.
2. Wise, J. J., Auto/oil air quality improvement research program, *in* "Spring Meeting of the AIChE, New Orleans, LA, 1992."
3. "Dow/Union Carbide Process for Mixed Alcohols from Syngas, in SRI PEP Review, March 1986."
4. Forzatti, P., Tronconi, E., and Pasquon, I., *Catal. Rev. Sci. Eng.* **33**, 109 (1991).
5. Nunan, J. G., Bogdan, C. E., Klier, K., Smith, K. J., Young, C.-W., and Herman, R. G., *J. Catal.* **116**, 195 (1989).
6. Nunan, J. G., Herman, R. G., and Klier, K., *J. Catal.* **116**, 222 (1989).
7. Smith, K. J., and Anderson, R. B., *Can. J. Chem. Eng.* **61**, 40 (1983).
8. Boz, I., Sahibzada, M., and Metcalfe, I., *Ind. Eng. Chem. Res.* **33**, 2021 (1994).
9. Calverley, E., and Smith, K., *Ind. Eng. Chem. Res.* **31**, 792 (1992).
10. Stiles, A., Chen, F., Harrison, J., Hu, X., Storm, D., and Yang, H., *Ind. Eng. Chem. Res.* **30**, 811 (1991).
11. Kiennemann, A., Idriss, H., Kieffer, R., Chaumette, P., and Durand, D., *Ind. Eng. Chem. Res.* **30**, 1130 (1991).
12. Vedage, G. A., Himelfarb, P. B., Simmons, G. W., and Klier, K., *Amer. Chem. Soc. Symp. Ser.* **279**, 295 (1985).
13. Tronconi, E., Ferlazzo, N., Forzatti, P., and Pasquon, I., *Ind. Eng. Chem. Res.* **26**, 2122 (1987).
14. Villa, P. L., DelPiero, G., Cipelli, A., Lietti, L., and Pasquon, I., *Appl. Catal.* **27**, 161 (1986).
15. Forzatti, P., Cristiani, C., Ferlazzo, N., Lietti, L., Tronconi, E., Villa, P. L., and Pasquon, I., *J. Catal.* **111**, 120 (1988).
16. Beretta, A., Sun, Q., Herman, R., and Klier, K., *Ind. Eng. Chem. Res.* **35**, 1534 (1996).
17. Tronconi, E., Lietti, L., Forzatti, P., and Pasquon, I., *Appl. Catal.* **47**, 317 (1989).
18. Epling, W. S., Hoflund, G. B., Nart, N. M., and Minahan, D. M., *J. Catal.* **169**, 438 (1997).
19. Campos-Martin, J. M., Fierro, J. L. G., Cuerrero-Ruiz, A., Herman, R. G., and Klier, K., *J. Catal.* **163**, 418 (1996).
20. Allen, G. C., Curtis, M. T., Hooper, A. J., and Tucker, P. M., *J. Chem. Soc. Dalton Trans.* **1677** (1973).
21. Wagner, C. D., Riggs, W. M., Davis, L. E., Moulder, J. F., and Muilenberg, G. E., "Handbook of X-ray Photoelectron Spectroscopy," Physical Electronics, Eden Prairie, MN, 1979.
22. Allen, G. C., and Tucker, P. M., *Inorg. Chim. Acta* **16**, 41 (1976).
23. Hoflund, G. B., and Epling, W. S., *Thin Solid Films* **292**, 236 (1997).